Solving Inverse Scattering for a Partially Immersed Metallic Cylinder Using Steady-State Genetic Algorithm and Asynchronous Particle Swarm Optimization by TE waves

Ching-Lieh Li [1], Chi Hsien Sun [2], Chien-Ching Chiu [1], and Lung-Fai Tuen [1]

[1] Electrical Engineering Department, Tamkang University
Tamsui, Taiwan, R.O.C

[2] Department of Electronic and Computer Engineering, National Taiwan University of Science and Technology, Taipei City, Taiwan, R.O.C.

Abstract ― The transverse electric (TE) polarization for shape reconstruction of a metallic cylinder by asynchronous particle swarm optimization (APSO) and steady-state genetic algorithm (SSGA) is presented. These approaches are applied to two-dimensional configurations. After an integral formulation, a discretization using the method of moment (MoM) is applied. Considering that the microwave imaging is recast as a nonlinear optimization problem, an objective function is defined by the norm of a difference between the measured scattered electric field and that calculated for an estimated shape of metallic cylinder. Thus, the shape of metallic cylinder can be obtained by minimizing the objective function. In order to solve this inverse scattering problem, two techniques are employed. The first is asynchronous particle swarm optimization. The second is steady-state genetic algorithm. Both techniques have been tested in the case of simulated measurements contaminated by additive white Gaussian noise. Numerical results indicate that the asynchronous particle swarm optimization outperforms steady-state genetic algorithm in terms of reconstruction accuracy and convergence speed.

Index Terms - Asynchronous particle swarm optimization, inverse scattering, partially immersed conductor, and transverse electric wave.

I. INTRODUCTION

Microwave imaging is an application of electromagnetic inverse scattering that is capable of performing noninvasive evaluation on a test object and determining its shape and/or material properties. The application of electromagnetic scattering to retrieve the shape, location, and the property of an unknown scatterer embedded in a homogeneous space or buried underground has shown great potential in several application areas such as medical tomography, geophysics, non-destructive testing, and object detection [1-11]. The reconstruction of the location, shape and/or size of metallic cylinders in a two-layer material medium may find its application for detection of landmine.

From a mathematical point of view, inverse problems are intrinsically ill-posed and nonlinear [12]. Hence, only a finite number of parameters can be accurately retrieved. To stabilize the inverse problems against ill-posedness, usually various kinds of regularizations are used, which are based on a priori information about desired parameters. On the other hand, due to the multiple scattering phenomena, the inverse-scattering problem is nonlinear in nature. Therefore, when multiple scattering effects are not negligible, the use of nonlinear methodologies is mandatory [13]. Recently, inverse scattering problems are usually considered in optimization-based procedures, such as adjoint-field scheme [14], Gauss–Newton method [15] genetic algorithms (GAs) [16-19], differential evolution (DE) [20-23], particle swarm

Submitted On: July 16, 2012
Accepted On: May 16, 2013

optimization (PSO) [23-28], and level-set algorithm [29]. However, these papers only focus on transverse magnetic (TM) cases.

It has been recognized that the 2D TE problems include two orthogonal electric field components in the transverse plane and thus leads to a vectorial mathematical formulation. Therefore, the computational load for exploiting such positive features is unavoidably increased as compared to the TM case with only one electric field component. In other words, the TE-polarized case includes polarization charges at dielectric discontinuities, which are more difficult to model numerically. However, there are advantages of utilizing the TE-polarized data (as compared to the TM-polarized ones) since they may contain more useful information about the object of interest data. It should be noted that these two polarizations are physically uncoupled and they provide independent information about the object being imaged [29, 30], although this may not be "practically" true when the curvature radius of the perfectly conducting cylinder is larger than the wavelength [31, 32].

Although particle swarm optimization and genetic algorithms have been confronted to numerical analysis and electromagnetic optimization problem [33-36], to the best of our knowledge, a comparative study about the performances of APSO and SSGA when applied to inverse scattering problems has not yet been investigated. Recently, there are a few reports on subject of 2D object about shape reconstruction problems by TE experimental data, such as genetic algorithms (GAs) [37-40] and level-set algorithm [29].

In this paper, the inverse scattering problem of the partially immersed perfectly conducting cylinder by TE wave illumination is investigated. We use the APSO to recover the shape of a partially immersed perfectly conducting cylinder. In section II, the theoretical formulation for the inverse scattering is derived. The numerical results for various objects of different shapes are presented in section III. Section IV gives the conclusions.

II. THEORETICAL FORMOLATION

A. Direct problem

Let us consider a perfectly conducting cylinder, which is partially immersed in a lossy homogeneous half-space, as shown in Fig. 1. Media in regions 1 and 2 are characterized by permittivities and conductivities (ε_1, σ_1) and (ε_2, σ_2), respectively. In our simulation, a priori information is assuming that scatterer is a metallic cylinder. A perfectly conducting cylinder is illuminated by a TE plane wave. The cylinder is of an infinite extent in the *z*-direction, and its cross-section is described in polar coordinates in the *x*, *y* plane by the equation $\rho = F(\theta)$. We assume that the time dependence of the field is harmonic with the factor $e^{j\omega t}$. Let $\vec{H}^{inc}$ denote the incidence field from region 1 with incident angle ϕ_1 as follow,

$$\vec{H}^{inc} = e^{-jk_1(y\cos\phi_1 + x\sin\phi_1)}\hat{z}. \qquad (1)$$

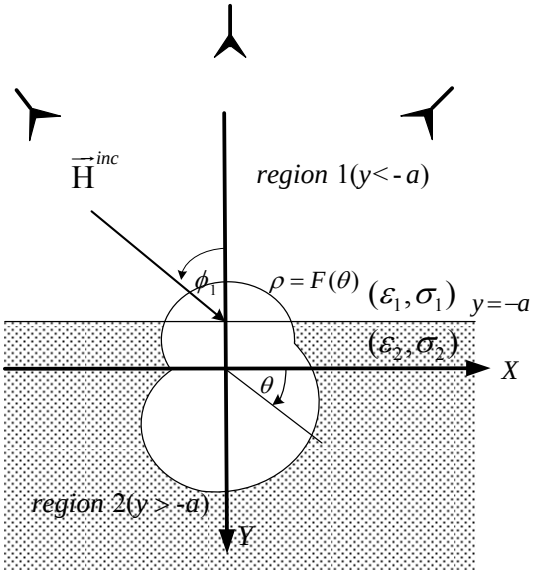

Fig. 1. Geometry of the problem in the (*x*,*y*) plane.

Owing to the interface between regions 1 and 2, the incident plane wave generates two waves that would exist in the absence of the conducting object. Since the cylinder is partially immersed, the equivalent current exists both in the upper half space and the lower half space. As a result, the details of Green's function are given first as follows:

(1) When the equivalent current exists in the upper half space, the Green's function for the line source in the region 1 can be expressed as,

$$G_1(x,y;x',y')=\begin{cases}G_{21}(x,y;x',y') & ,y>-a\\ G_{11}(x,y;x',y')= & \\ G_{f11}(x,y;x',y')+G_{s11}(x,y;x',y') & ,y\le -a\end{cases}$$

$$G_{21}(x,y;x',y')=\frac{1}{2\pi}\int_{-\infty}^{\infty}\frac{j}{\gamma_1+\gamma_2}e^{-j\gamma_2(y+a)}e^{j\gamma_1(y'+a)}e^{-j\alpha(x-x')}d\alpha$$

$$G_{f11}(x,y;x',y')=\frac{j}{4}H_0^{(2)}[k_1\sqrt{(x-x')^2+(y-y')^2}]\ , \tag{2.2}$$

$$G_{s11}(x,y;x',y')=\frac{1}{2\pi}\int_{-\infty}^{\infty}\frac{j}{2\gamma_1}(\frac{\gamma_1-\gamma_2}{\gamma_1+\gamma_2})e^{j\gamma_1(y+2a+y')}e^{-j\alpha(x-x')}d\alpha \tag{2.3}$$

$\gamma_i^2=k_i^2-\alpha^2$, $i=1,2,\ \mathrm{Im}(\gamma_i)\le 0, y'<-a$.

(2) When the equivalent current exists in the lower half space, the Green's function for the line source in the region 2, is

$$G_2(x,y;x',y')=\begin{cases}G_{12}(x,y;x',y') & ,y\le -a\\ G_{22}(x,y;x',y')= & \\ G_{f22}(x,y;x',y')+G_{s22}(x,y;x',y'), & y>-a\end{cases} \tag{3}$$

where

$$G_{12}(x,y;x',y')=\frac{1}{2\pi}\int_{-\infty}^{\infty}\frac{j}{\gamma_1+\gamma_2}e^{j\gamma_1(y+a)}e^{-j\gamma_2(y'+a)}e^{-j\alpha(x-x')}d\alpha\ , \tag{3.1}$$

$$G_{f22}(x,y;x',y')=\frac{j}{4}H_0^{(2)}[k_2\sqrt{(x-x')^2+(y-y')^2}]\ , \tag{3.2}$$

$$G_{s22}(x,y;x',y')=\frac{1}{2\pi}\int_{-\infty}^{\infty}\frac{j}{2\gamma_2}(\frac{\gamma_2-\gamma_1}{\gamma_2+\gamma_1})e^{-j\gamma_2(y+y'+2a)}e^{-j\alpha(x-x')}d\alpha\ , \tag{3.3}$$

$\gamma_i^2=k_i^2-\alpha^2$, $i=1,2,\ \mathrm{Im}(\gamma_i)\le 0, y'>-a$.

For programming purposes, the scattered magnetic field can be expressed according to the following two cases,

[case 1] if $a>0$ ($\theta_1>\theta_2$)

$$H^S(\vec{r})=\begin{cases}H_1^S(\vec{r})= & \\ \int_{\theta_1-2\pi}^{\theta_2}G_{12}(x,y;x',y')J_m(\theta')d\theta' & \\ +\int_{\theta_2}^{\theta_1}G_{11}(x,y;x',y')J_m(\theta')d\theta', & y\le -a\\ H_2^S(\vec{r})= & \\ \int_{\theta_1-2\pi}^{\theta_2}G_{22}(x,y;x',y')J_m(\theta')d\theta' & \\ +\int_{\theta_2}^{\theta_1}G_{21}(x,y;x',y')J_m(\theta')d\theta', & y>-a\end{cases} \tag{4}$$

[case 2] if $a<0$ ($\theta_1<\theta_2$)

$$H^s(\vec{r})=\begin{cases}H_1^S(\vec{r})= & \\ \int_{\theta_1}^{\theta_2}G_{12}(x,y;x',y')J_m(\theta')d\theta' & \\ +\int_{\theta_2}^{2\pi-\theta_1}G_{11}(x,y;x',y')J_m(\theta')d\theta', & y\le -a\\ H_2^S(\vec{r})= & \\ \int_{\theta_1}^{\theta_2}G_{22}(x,y;x',y')J_m(\theta')d\theta' & \\ +\int_{\theta_2}^{2\pi-\theta_1}G_{21}(x,y;x',y')J_m(\theta')d\theta', & y>-a\end{cases} \tag{5}$$

with

$$J_m(\theta)=-j\omega\varepsilon\sqrt{F^2(\theta)+F'^2(\theta)}J_{sm}(\theta)\ .$$

Here, $J_{sm}(\theta)$ is the induced surface magnetic current density, which is proportional to the normal derivative of the magnetic field on the conductor surface. $G_1(x, y; x', y')$ and $G_2(x, y; x', y')$ denote the Green's function for the line source in regions 1 and 2, respectively. $H_0^{(2)}$ is the Hankel function of the second kind of order zero. We might face some difficulties in calculating the Green's function. The Green's function, given by equation (2), is in the form of an improper integral, which must be evaluated numerically. However, the integral converges very slowly when r and r' approach the interface $y = -a$. Fortunately, we find that the integral in G_1 or G_2 may be rewritten as a closed-form term plus a rapidly converging integral. Thus the whole integral in the Green's function can be calculated efficiently.

For a perfectly conducting scatterer, the total tangential electric field at the surface of the scatterer is equal to zero,

$$\hat{n} \times (\frac{1}{j\omega\varepsilon} \nabla \times \vec{H}^{tot}) = 0 \qquad (6)$$

with $\vec{H}^{tot} = \vec{H}^{i} + \vec{H}^{s}$, where $\hat{n}$ is the outward unit vector normal to the surface of the scatterer and $\vec{H}^{s}$ is the scattered field. For the direct scattering problem, the scattered field $\vec{H}^{s}$ is calculated by assuming that the shape is known. For the inverse problem, assume the approximate center of scatterer, which in fact can be any point inside the scatterer, is known. Then the shape function $F(\theta)$ can be expanded as,

$$F(\theta) = \sum_{n=0}^{N/2} B_n \cos(n\theta) + \sum_{n=1}^{N/2} C_n \sin(n\theta) \qquad (7)$$

where B_n and C_n are real coefficients to be determined, and N+1 is the number of unknowns for the shape function. In the inversion procedure, the asynchronous particle swarm optimization is used to minimize the following cost function [36],

$$CF = \{\frac{1}{M_t} \sum_{m=1}^{M_t} \left|\vec{H}^{s}_{exp}(\vec{r}_m) - \vec{H}^{s}_{cal}(\vec{r}_m)\right|^2 / \left|\vec{H}^{s}_{exp}(\vec{r}_m)\right|^2\}^{1/2} \qquad (8)$$

where M_t is the total number of measurement points. $\vec{H}^{s}_{exp}(\vec{r}_m)$ and $\vec{H}^{s}_{cal}(\vec{r}_m)$ are the measured and calculated scattered fields, respectively.

B. Asynchronous particle swarm optimization (APSO)

APSO starts with an initial population of potential solutions that is composed by a group of randomly generated individuals. Each individual is a D-dimensional vector consisting of D optimization parameters. The initial population may be expressed by $\{X_j: j = 1, 2, ..., N_p\}$, where N_p is the population size. Clerc [41] suggested the use of a different velocity update rule, which introduced a parameter ξ called constriction factor. The role of the constriction factor is to ensure convergence when all the particles tend to stop their movement. The flow chart of the APSO algorithm is shown in Fig. 2. The velocity update rule is then given by,

$$v_j^{k+1} = \xi \cdot \left(v_j^k + c_1 \cdot \phi_1 \cdot \left(x^k_{pbest_j} - x_j^k\right) + c_2 \cdot \phi_2 \cdot \left(x^k_{gbest} - x_j^k\right)\right), \qquad (9)$$

$$x_j^{k+1} = x_j^k + v_j^{k+1},\ j = 0 \sim N_p - 1, \qquad (10)$$

where $\xi = \dfrac{2}{\left|2 - \phi - \sqrt{\phi^2 - 4\phi}\right|}$, $\phi = c_1 + c_2 \geq 4$.

The symbols c_1 and c_2 are the learning coefficients used to control the impact of the local and global component in the velocity term of equation (9), ξ is the constriction factor, ϕ_1 and ϕ_2 are both random numbers between 0 and 1.

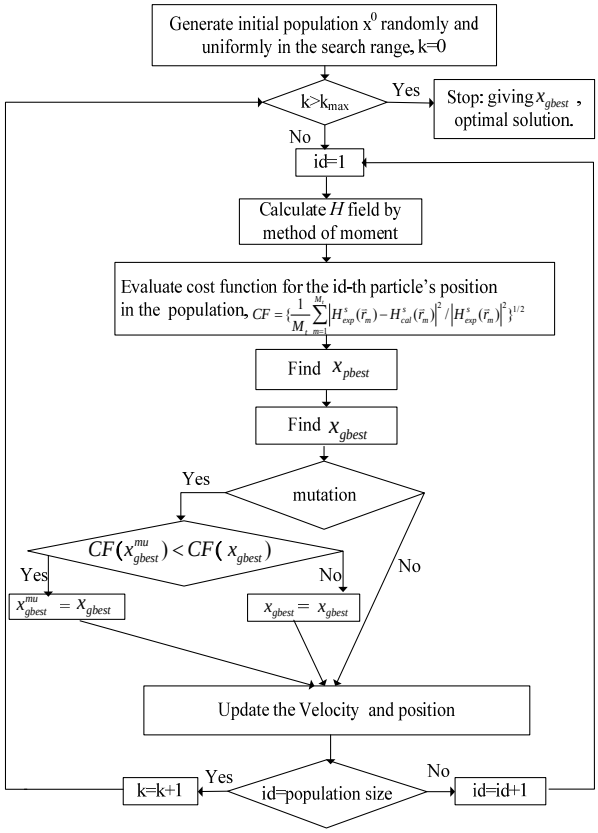

Fig. 2. The flowchart of the modified asynchronous PSO (APSO).

The key distinction between a particle swarm optimization (PSO) and the asynchronous particle swarm optimization (APSO) is on the updating mechanism, damping boundary condition and mutation scheme. The current updating mechanism of asynchronous PSO use the following rule: just after the update of equation (9) for each particle the best positions x_{pbest} and x_{gbest} will be replaced if the new position is better than the current best ones such that they can be used immediately for the next particle. In this way, the swarm reacts more quickly to speed up the convergence.

Boundary conditions in PSO play a key role as it is pointed out in [42]. In this paper we have applied the damping boundary condition and mutation scheme. The mutation scheme plays a role in avoiding premature convergences for the searching procedure and helps the x_{gbest} escape from the local optimal position. More details about the APSO algorithm can be found in [28].

III. Numerical Results

We illustrate the performance of the proposed inversion algorithm and its sensitivity to random noise in the scattered field. Let us consider a perfectly conducting cylinder buried in a lossless half-space ($\sigma_1 = \sigma_2 = 0$). The permittivity in each region is characterized by $\varepsilon_1 = \varepsilon_0$ and $\varepsilon_2 = 2.7\ \varepsilon_0$, respectively. The frequency of the incident wave is chosen to be 3 GHz with incident angles ϕ_l equals to - 45^0, 0^0, and 45^0, respectively. The wavelength λ_0 is 0.5 m. The purpose of this study is to reconstruct the shape of the partially immersed perfectly conducting cylinder by using the scattered fields at different incident angles. To reconstruct the shape of the cylinder, the object is illuminated by incident waves from three different directions and 8 measurements are made for each incident angle at the points equally separated on a semi-circle with the radius of 3 m in region 1 along the interface $y = -a$, which is considered here as a test configuration for future application of landmine detection. To save computing time, the number of unknowns is set to be 7. Moreover, to avoid inverse crime, the discretization number for the direct problem is two times that for the inverse problem in the simulation. In forward problem, the shape function $F(\theta)$ is discretized to 60. The related coefficients of the APSO are set below. The learning coefficients c_1 and c_2 are set to 2.8 and 1.3, respectively [43]. The mutation probability is 0.1 and the population size is set to 70. The operations coefficients for the NU-SSGA algorithm are set as below: The crossover probability and the mutation probability are set to be 0.02 and 0.05, respectively [19]. The population size N_p is the same with APSO. The searching range for the unknown coefficients is chosen from 0 to 1.0. The relative error of shape function (RE) of the reconstructed shape is defined as,

$$RE = \{\frac{1}{N'}\sum_{i=1}^{N'}[\vec{F}^{cal}(\theta_i) - \vec{F}(\theta_i)]^2 / \vec{F}^2(\theta_i)\}^{1/2} \ . \tag{11}$$

where N' is cutting number of the object. $F^{cal}(\theta_i)$ and $F(\theta_i)$ are calculated shape function and is given the shape function.

In the first example, the shape function is chosen to be $F(\theta) = (0.1 + 0.04\cos 2\theta)$ m. In this case, the final reconstructed shapes by NU-SSGA algorithm and APSO scheme at the 1000 th generation are compared to the exact shape in Fig. 3. Figure 4 shows that the reconstruction relative error versus the number of iterations by NU-SSGA algorithm and APSO, respectively. It is clear that the APSO outperforms NU-SSGA.

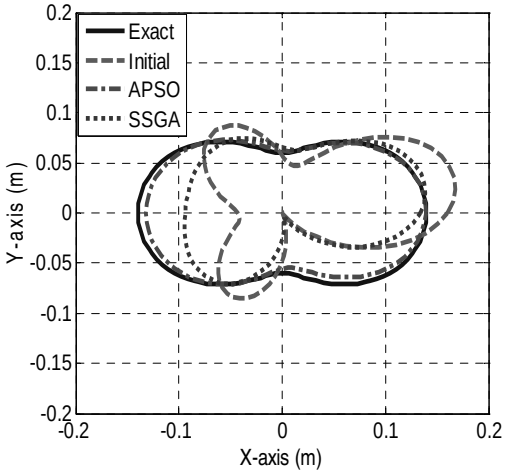

Fig. 3. The reconstructed shape of the cylinder for example 1.

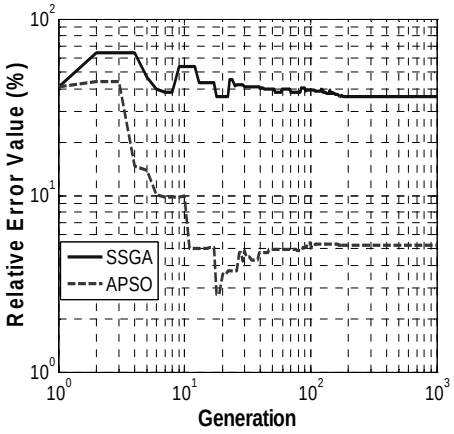

Fig. 4. Shape function error in each generation.

In the second example, the shape function is chosen to be $F(\theta) = (0.1 + 0.03\cos 2\theta + 0.025\sin 2\theta + 0.015\sin 3\theta)$ m. The reconstructed shape function for the best population member is plotted in Fig. 5 with the shape error shown in Fig. 6. The reconstructed shape error is 5.3 % by APSO and it is seen that the error comes from the bottom of the shape. It is noted that the APSO still outperforms NU-SSGA in term of reconstruction accuracy and convergence speed.

For investigating the effect of noise, we add to each complex scattered field a quantity $b+cj$, where b and c are independent random numbers having a Gaussian distribution with zero mean, each random number is multiplied by the noise level times the rms value of the scattered field. The SNR applied include 40 dB, 30 dB, 20 dB, 10 dB, and 5 dB in the simulations. The numerical results for examples 1 and 2 are plotted in Fig. 7. They show that the effect of the noise is tolerable for noise levels below 10 dB.

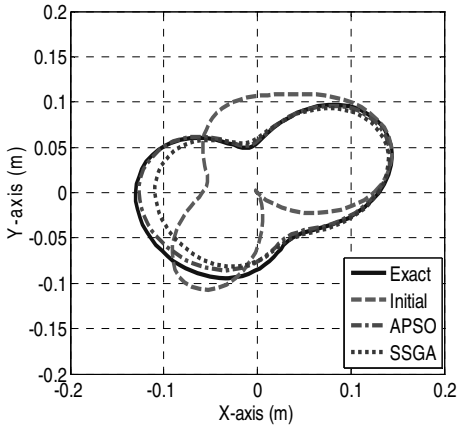

Fig. 5. The reconstructed shape of the cylinder for example 2.

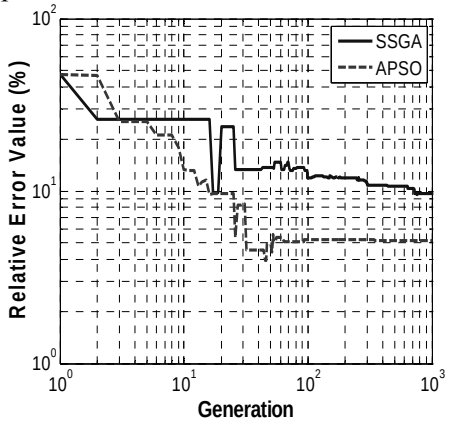

Fig. 6. Shape function error in each generation.

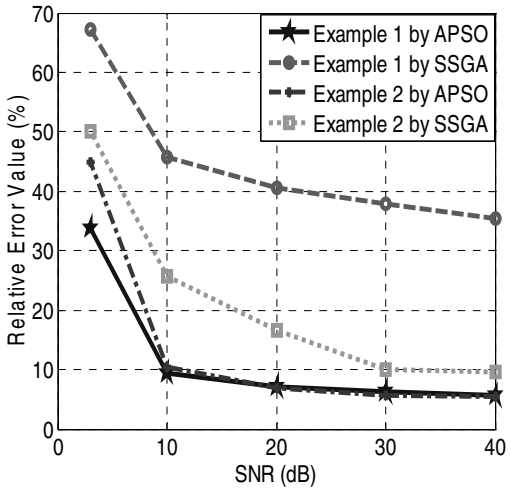

Fig. 7. Shape function error as a function of SNR for all examples.

IV. CONCLUSION

We have presented a study of applying the APSO and NU-SSGA to reconstruct the shapes of a partially immersed conducting cylinder illuminated by TE waves. The inverse problem is reformulated into an optimization one. Numerical results show that the APSO has better reconstructed results compared with NU-SSGA when the same number of iterations is applied.

Some numerical examples have been given, and good agreement between the exact and the reconstructed profiles is achieved by APSO in each case. The effect of noise on the overall reconstruction has also been investigated, and it is observed that the proposed method is able to provide good shape reconstruction as long as the normalized SNR is > 10 dB.

ACKNOWLEDGEMENT

This work was supported by the National Science Council, Republic of China, under Grant NSC 101-2221-E-032-029.

REFERENCES

[1] T. Takenaka and T. Moriyama, "Inverse scattering approach based on the field equivalence principle: inversion without a priori information on incident fields," *Optics Letters*, vol. 37, pp. 3432-3434, Aug. 2012.

[2] F. Soldovieri, F. Ahmad, and R. Solimene, "Validation of microwave tomographic inverse scattering approach via through-the-wall experiments in semi controlled conditions," *IEEE*

Transactions Geoscience and Remote Sensing, vol. 8, no. 1, pp. 123-127, Jan. 2011.

[3] C. H. Sun, C. L. Li, C. C. Chiu, and C. H. Huang, "Time domain image reconstruction for a buried 2D homogeneous dielectric cylinder using NU-SSGA," *Research in Nondestructive Evaluation,* vol. 22, no.1, pp. 1-15, Jan. 2011.

[4] C. C. Chiu, C. H. Sun, C. L. Li, and C. H. Huang, "Comparative study of some population-based optimization algorithms on inverse scattering of a two-dimensional perfectly conducting cylinder in slab medium," *IEEE Transactions on Geoscience and Remote Sensing*, vol. 51, pp. 2302-2315, Apr. 2013.

[5] M. Benedetti, D. Lesselier, M. Lambert, and A. Massa, "Multiple-shape reconstruction by means of multiregion level sets," *IEEE Transactions Geoscience and Remote Sensing*, vol. 48, no. 5, pp. 2330-2342, May 2010.

[6] C. L. Li, C. H. Huang, C. C. Chiu, and C. H. Sun, "Comparison of dynamic differential evolution and asynchronous particle swarm optimization for inverse scattering of a two-dimensional perfectly conducting cylinder," *Applied Computational Electromagnetics Society (ACES) Journal*, vol. 27, no. 10, pp. 850-865, October 2012.

[7] Z. Zhang, Z. Zhu, Q. Xin, X. Xie, J. Lei, and S. Huang, "Analysis and application of inverse detecting method based on local electric field," *Applied Computational Electromagnetics Society (ACES) Journal*, vol. 27, no. 7, pp. 566-573, July 2012.

[8] C. Huang, C. Chen, C. Chiu, and C. Li, "Reconstruction of the buried homogenous dielectric cylinder by FDTD and asynchronous particle swarm optimization," *Applied Computational Electromagnetics Society (ACES) Journal*, vol. 25, no. 8, pp. 672-681, August 2010.

[9] C. H. Sun, C. C. Chiu, and C. H. Chen "Time domain microwave imaging for a metallic cylinder by using evolutionary algorithms," *Imaging Science Journal*, vol. 61, pp. 3-12, Jan. 2013.

[10] M. Farmahini-Farahani, R. Faraji-Dana, and M. Shahabadi, "Fast and accurate cascaded particle swarm gradient optimization method for solving 2-D inverse scattering problems," *Applied Computational Electromagnetics Society (ACES) Journal*, vol. 24, no. 5, pp. 511-517, October 2009.

[11] C. H. Huang, C. C. Chiu, C. J. Lin, and Y. F. Chen, "Inverse scattering of inhomogeneous dielectric cylinders buried in a slab medium by TE wave illumination," *Applied Computational Electromagnetics Society (ACES) Journal*, vol. 22, no. 2, pp. 295-301, July 2007.

[12] P. C. Sabatier, "Theoretical considerations for inverse scattering," *Radio Science*, vol. 18, pp. 629-631, 1983.

[13] A. M. Denisov, *Elements of Theory of Inverse Problems*, VSP, Utrecht, The Netherlands, 1999.

[14] M. El-Shenawee, O. Dorn, and M. Moscoso, "An adjoint-field technique for shape reconstruction of 3-D penetrable object immersed in lossy medium," *IEEE Trans. Antennas Propag*., vol. 57, no. 2, pp. 520-534, 2009.

[15] T. Rubaek, P. M. Meaney, P. Meincke, and K. D. Paulsen, "Nonlinear microwave imaging for breast-cancer screening using Gauss-Newton's method and the CGLS inversion algorithm," *IEEE Trans. Antennas Propag*., vol. 55, no. 8, pp. 2320-2331, 2007.

[16] C. H. Sun, C. L. Li, C. C. Chiu, and C. H. Huang, "Time domain image reconstruction for a buried 2D homogeneous dielectric cylinder using NU-SSGA," *Research in Nondestructive Evaluation,* vol. 22, no.1, pp. 1-15, Jan. 2011.

[17] W. Chien, C. H. Sun, and C. C. Chiu, "Image reconstruction for a partially immersed imperfectly conducting cylinder by genetic algorithm," *International Journal of Imaging Systems and Technology*, vol. 19, pp. 299-305, 2009.

[18] X. M. Zhong, C Liao, and W. Chen, "Image reconstruction of arbitrary cross section conducting cylinder using UWB pulse," *Journal of Electromagnetic Waves Application*, vol. 21, no. 1, pp. 25-34, 2007.

[19] W. Chien and C. C. Chiu, "Using NU-SSGA to reduce the searching time in inverse problem of a buried metallic object," *IEEE Transactions on Antennas and Propagation*, vol. 53, no. 10, pp. 3128-3134, 2005.

[20] K. A. Michalski, "Electromagnetic imaging of circular-cylindrical conductors and tunnels using a differential evolution algorithm," *Microwave and Optical Technology Letters*, vol. 27, no. 5, pp. 330-334, Dec. 2000.

[21] A. Semnani, I. T. Rekanos, M. Kamyab, and M. Moghaddam, "Solving inverse scattering problems based on truncated cosine Fourier and cubic B-spline expansions," *IEEE Transactions on Antenna Propagation*, vol. 60, pp. 5914-5923, Dec. 2012.

[22] C. H. Sun, C. C. Chiu, C. L. Li, and C. H. Huang, "Time domain image reconstruction for homogenous dielectric objects by dynamic differential evolution," *Electromagnetics*, vol. 30, no. 4, pp. 309-323, May 2010.

[23] A. Semnani, I. T. Rekanos, M. Kamyab, and T. G. Papadopoulos, "Two-dimensional microwave imaging based on hybrid scatterer representation and differential evolution," *IEEE Trans. Antennas*

Propag., vol. 58, no. 10, pp. 3289-3298, Oct. 2010.

[24] I. T. Rekanos, "Shape reconstruction of a perfectly conducting scatterer using differential evolution and particle swarm optimization," *IEEE Transactions on Geoscience and Remote Sensing*, vol. 46, no. 7, pp. 1967-1974, 2008.

[25] A. Semnani and M. Kamyab, "An enhanced hybrid method for solving inverse scattering problems," *IEEE Transactions on Magnetics*, vol. 45, no. 3, pp. 1534-1537, March 2009.

[26] C. H. Chen, C. C. Chiu, C. H. Sun, and W. L. Chang, "Two-dimensional finite-difference time domain inverse scattering scheme for a perfectly conducting cylinder," *Journal of Applied Remote Sensing,* vol. 5, 053522, May 2011.

[27] M. Donelli and A. Massa, "Computational approach based on a particle swarm optimizer for microwave imaging of two-dimensional dielectric scatterers," *IEEE Transactions on Microwave Theory and Techniques*, vol. 53, no. 5, pp. 1761-1776, May 2005.

[28] C. C. Chiu, C. H. Sun, and W. L. Chang "Comparison of particle swarm optimization and asynchronous particle swarm optimization for inverse scattering of a two-dimensional perfectly conducting cylinder," *International Journal of Applied Electromagnetics and Mechanics*, vol. 35, no. 4, pp. 249-261, April 2011.

[29] M. R. Hajihashemi and M. E. Shenawee, "TE versus TM for the shape reconstruction of 2-D PEC targets using the level-set algorithm," *IEEE Transactions on Geoscience and Remote Sensing*, vol. 48, no. 3, pp. 1159-1168, 2010.

[30] A. Litman, "Reconstruction by level sets of n-array scattering obstacles," *Inverse Probl.*, vol. 21, no. 6, pp. S131-S152, Dec. 2005.

[31] A. Liseno, R. Pierri, and F. Soldovieri, "Shape identification by physical-optics: the two-dimensional TE case," *J. Opt. Soc. Am. A*, vol. 20, no. 9, pp. 1827-1830, Sept. 2003.

[32] C. L. Li, S. H. Chen, C. M. Yang, and C. C. Chiu, "Electromagnetic imaging for a partially immersed perfectly conducting cylinder by the genetic algorithm," *Radio Science*, vol. 39, no. 2, RS2016, April 2004.

[33] R. C. Eberhart and Y. Shi, "Comparison between genetic algorithms and particle swarm optimization," *Proc. 7th Annu. Conf. Evol. Program (EP-98)*, vol. 1447, pp. 611-616, Lecture Notes in Computer Science, March 1998.

[34] R. J. W. Hodgson, "Particle swarm optimization applied to the atomic cluster optimization problem," *Proc. Genetic and Evol. Comp. Conf.* (GECCO-2002), pp. 68-73, 2002.

[35] R. Hassan, B. Cohanim, and O. de Weck, "A comparison of particle swarm optimization and the genetic algorithm," *Proc. of the 46th AIAA/ASME/ASCE/AHS/ASC Structures, Structural Dynamics, and Materials Conference*, pp. 1-13, 2005.

[36] D. W. Boeringer and D. H. Werner, "Particle swarm optimization versus genetic algorithms for phased array synthesis," *IEEE Transactions on Antenna Propagation*, vol. 52, pp. 771-779, March 2004.

[37] J. Ma, W. C. Chew, C. C. Lu, and J. Song, "Image reconstruction from TE scattering data using equation of strong permittivity fluctuation," *IEEE Trans. Antennas Propag*. vol. 48, no. 6, pp. 860-867, 2000.

[38] C. H. Sun, C. L. Liu, K. C. Chen, C. C. Chiu, C. L. Li, and C. C. Tasi, "Electromagnetic transverse electric wave inverse scattering of a partially immersed conductor by steady-state genetic algorithm," *Electromagnetics*, vol. 28, no. 6, pp. 389-400, Aug. 2008.

[39] Y. C. Chen, Y. F. Chen, C. C. Chiu, and C. Y Chang, "Image reconstruction of buried perfectly cylinder illuminated by transverse electric waves," *International Journal of Imaging Systems and Technology*, vol. 15, pp. 261-265, 2006.

[40] Y. S. Lin and C. C. Chiu, "Image reconstruction for a perfectly conducting cylinder buried in slab medium by a TE wave illumination," *Electromagnetics*, vol. 25, no. 3, pp. 203-216, 2005.

[41] M. Clerc, "The swarm and the queen: towards a deterministic and adaptive particle swarm optimization," *Proceedings of Congress on Evolutionary Computation*, pp. 1951 - 1957, 1999.

[42] T. Huang and A. S. Mohan, "A hybrid boundary condition for robust particle swarm optimization," *IEEE Antennas and Wireless Propagation Letters*, vol. 4, pp. 112 - 117, 2005.

[43] A. Carlisle and G. Dozier, "An off-the-shelf PSO," *Proceedings of the 2001 Workshop on Particle Swarm Optimization*, pp. 1-6, 2001.

Ching-Lieh Li was born November 24, 1963, in Pingtun, Taiwan. He received the B.Sc. degree from National Taiwan University, Taipei, Taiwan, in 1985, and the M.Sc. and Ph.D. degrees from Michigan State University, East Lansing, in 1990 and 1993, respectively, all in

Electrical Engineering.

From 1989 to 1993, he was a Research Assistant in the Electrical Engineering Department, Michigan State University, where he worked on the measurement techniques for determining the electromagnetic properties of materials. In 1993, he joined the Electrical Engineering Faculty at Tamkang University, Taipei, Taiwan, where now he is a professor. Currently, his research activities involve inverse scattering problem, and microstrip antenna design and dielectric material characterization, etc. His areas of special interest include theoretical and computational electromagnetics, and application of various optimization schemes such as SSGA, PSO, DE, and Taguchi method to electromagnetics.

Chi-Hsien Sun received MSEE and PhD degrees in Electrical Engineering from Tamkang University, Taipei, Taiwan, in 2008 and 2012, respectively. Since 2012, he has been a postdoctoral with the Department of Electronic and Computer Engineering,National Taiwan University of Science and Technology. His special interests include radio over fiber (ROF), WDM-PON and computational electromagnetics, and application of various optimization schemes such as the steady state genetic algorithm (SSGA), particle swarm optimization (PSO), dynamic differential evolution (DDE), self-adaptive dynamic differential evolution (SADDE), and the Taguchi method in electromagnetics

Chien-Ching Chiu received his B.Sc. degree from National Chiao Tung University, Hsinchu, Taiwan, in 1985 and his M.Sc. and PhD degrees from National Taiwan University, Taipei, in 1987 and 1991, respectively. From 1987 to 1989, he was a communication officer with the ROC Army Force. In 1992 he joined the faculty of the Department of Electrical Engineering, Tamkang University, where he is now a professor. From 1998 to 1999, he was a visiting scholar at the Massachusetts Institute of Technology, Cambridge, and the University of Illinois at Urbana-Champaign. He is a visiting professor with the University of Wollongong, Australia, in 2006. Moreover, he was a visiting professor with the University of London, United Kingdom, in 2011. His current research interests include microwave imaging, numerical techniques in electromagnetics, indoor wireless communications, and ultra wideband communication systems. He has published more than 90 journal papers on inverse scattering problems, communication systems and optimization algorithms.

Lung-Fai Tuen received the B.Sc. degree from Jinwen University of Science and Technology, Taipei, Taiwan, in 2006, and the M.Sc. degree and Ph.D. student from Tamkang University, in 2009 and 2013, respectively, all in Electrical Engineering. From 2007 to 2009, he was a Research Assistant in the Electrical Engineering Department, Tamkang University, where he worked on the development techniques for array antenna design.